Wind turbine noise propagation modelling: An unsteady approach

Barlas, Emre; Zhu, Wei Jun; Shen, Wen Zhong; Andersen, Søren Juhl

Published in:
Journal of Physics: Conference Series (Online)

Link to article, DOI:
10.1088/1742-6596/753/2/022003

Publication date:
2016

Document Version
Publisher's PDF, also known as Version of record

Wind Turbine Noise Propagation Modelling: An Unsteady Approach

E Barlas, W J Zhu, W Z Shen and S J Andersen
DTU Wind Energy, Technical University of Denmark, 2800 Kongens Lyngby, Denmark
E-mail: ebarlas@dtu.dk

Abstract.
Wind turbine sound generation and propagation phenomena are inherently time dependent, hence tools that incorporate the dynamic nature of these two issues are needed for accurate modelling. In this paper, we investigate the sound propagation from a wind turbine by considering the effects of unsteady flow around it and time dependent source characteristics. For the acoustics modelling we employ the Parabolic Equation (PE) method while Large Eddy Simulation (LES) as well as synthetically generated turbulence fields are used to generate the medium flow upon which sound propagates. Unsteady acoustic simulations are carried out for three incoming wind shear and various turbulence intensities, using a moving source approach to mimic the rotating turbine blades. The focus of the present paper is to study the near and far field amplitude modulation characteristics and time evolution of Sound Pressure Level (SPL).

1. Introduction

Even though the sound levels at certain distances from a wind turbine may be relatively low, the annoyance levels are observed to be higher than many other noise sources. This is attributed to the special characteristics of the wind turbine noise. The aerodynamic sound emitted from wind turbines constantly vary due to the unsteadiness of the incoming flow and the rotation of the blades. This results in both near and far field amplitude modulations in sound pressure levels (SPL), (see [1] for mechanisms of amplitude modulation). This unsteady nature of wind turbine noise causes annoyance even though the mean levels comply with the standards [2]. Hence an accurate modelling tool that is capable of capturing these dynamics is highly needed.

Previous work on the topic, carried out by the authors [3] showed that the sound propagation behind a wind turbine is significantly modified by the wake. Due to the wind speed deficit the sound waves are ducted within the wake and when the wake breaks down the so-called downwards bursting zones appear. These are the areas where the ground level receiver is exposed to higher noise levels as a result of severe downwards refraction. The present work employs a similar approach by coupling the solution from high resolution Large Eddy Simulation (LES) with the Parabolic Equation (PE) method. Additionally, synthetically generated turbulence is used for the upwind propagation. Using the varying flow input, the frequency dependent acoustic simulations are carried out successively allowing one to observe the time evolution of SPL. Three different wind shears are simulated and for each case various turbulence intensities are considered. All cases yield a different wind speed distribution, thus changing the refraction patterns of sound waves.

2. Computational Models

2.1. ***Model for the Sound Propagation***

There are various sound propagation models that come along with different benefits and drawbacks. We are interested in a model that is capable of handling range varying wind fields with a reasonable required computational power. Therefore, two-dimensional PE method was chosen as a compromise between accuracy and computational resources. The PE method is a solution of the wave equation with the approximations of harmonic wave, far field, finite angle and forward propagation. The conventional method uses the effective sound speed approach where the moving atmosphere is replaced by a hypothetical motionless medium with the effective sound speed $c_{eff} = c + v_x$, where v_x is the wind velocity component along the direction of propagation between source and receiver. With these assumptions the equation yields:

$$[\nabla^2 + k^2(1+\epsilon)]P'(r) = 0 \tag{1}$$

where $k = \omega/c_0$ (ω is the radian frequency of the sound, c_0 is the reference speed of sound), $P'(r)$ is the monochromatic sound field, $\epsilon = (c_0/c_{eff})^2 - 1$. Further mathematical manipulation in order to reduce these equations to one way parabolic equation is carried out in [4].

In this study semi-implicit marching scheme is used, with central differences scheme used in the vertical direction (z) and Crank-Nicolson method applied in the horizontal direction (x). The spatial resolution for both directions is set to one eighth of the wavelength ($\Delta x = \Delta z = \lambda/8$; where λ is the wavelength of the considered frequency). Only flat terrain is considered and the ground impedance was characterized using the Delany-Bazley model [5], with an effective flow resistivity of 200 kPas/m^2. All simulations are carried out for 1/3-octave band centre frequencies up to 800 Hz and summed logarithmically to obtain overall SPL: $Lp_{sum} = 10log_{10}\Big(\sum_{i=1}^{N} 10^{Lp(f_i)/10}\Big)$ where N is the number of frequencies used and $L_p(f_i)$ is the sound pressure level defined as:

$$L_p(f_i) = L_W(f_i) - 10log_{10}4\pi R^2 - \alpha R + \Delta L \tag{2}$$

where the source power level for a wind turbine (L_W) is obtained from the semi-empirical model explained in [6] (see also next section), the second term on the right hand side stands for geometrical spreading, the third term represents the atmospheric absorption where the absorption coefficient is calculated according to ISO 9613-1 for air at 20°C with 80% relative humidity. The last term is the relative sound pressure level $\Delta L = 10log_{10}(|P'|\,/\,|P_f|)$ that represents the deviation from the free field of a source due to ground effect, atmospheric refraction, turbulence etc. This last term is calculated using the PE method.

2.2. ***Model for the Wind Turbine as a Sound Source***

The dynamic nature of the wind turbine as a sound source is taken into account via a *moving source approach*. Taking advantage of the source location studies carried out in [7] a wind turbine can be treated as lumped sources located near the tips, i.e., at 85 % of the blade span. This helps to reduce a complex 3D source to three incoherent sources rotating with the blades. In such case a wind turbine that is rotating in and out of the 2D PE plane intersects the domain at the bottom and the top tip heights. Thus we model it via a point source that is translated either up or down at each time step taking the turbine rotational speed into account (see sec. 2.3). This is a good way to mimic the dynamics of a rotating wind turbine since the modulation due to blade passage is also captured. The point source starters are weighted with a different spectra at each time step that are obtained from the semi-empirical source model explained in [6]. Fig 1 shows a sample spectrogram for three different turbulence intensity (TI) while all other parameters remain same. A clear increase of SPL in the low frequency range with an increasing

TI is observed. The effect of this on far field noise propagation will be further investigated later in order to assess the importance of source modelling.

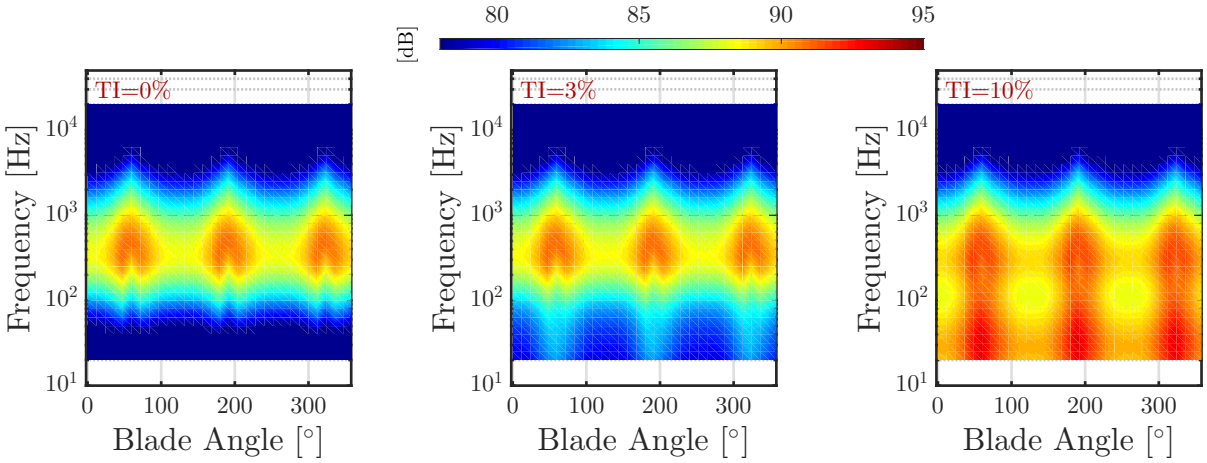

Figure 1. Source power level spectra for the NM80 turbine over one rotation obtained from the model in [6]. **From left to right:** Increasing the turbulence intensity (0%, 3%, 10%)

2.3. ***Models for the Flow Field Input***

Two different techniques were used to obtain the flow field input. For the downwind propagation the flow fields were obtained from high resolution LES. LES is performed using the 3D flow solver EllipSys3D, which was developed as a collaboration between Technical University of Denmark ([8]) and Risø National Laboratory ([9]). The influence of the wind turbine is simulated using the Actuator Line technique (for further details see [10]), which imposes body forces along the rotating lines. The body forces are calculated through a full aero-elastic coupling with Flex5, which computes the aerodynamic loads, see [11] for details on Flex5 and [12] for details on the coupling. The actuator line method relies on airfoil data, and the used 2D airfoil data have been corrected to take 3D rotational effects into account. The fully coupled simulations also include a controller, which means the simulated turbine behaves as a real turbine and adjusts according to the incoming turbulent flow field. The modelled turbine is the NM80 equipped with a large generator of 2.75MW (see [13]). The blade radius is $R = 40$ m and the rated power is 2.75 MW at rated wind speed of 14 m/s. The computational domain used for this study is [40 D X 10 D X 10 D] in the streamwise, vertical and lateral directions, respectively (D represents the turbine diameter, 80 m) and the turbine is located at 400 m from the inlet. The spatial resolution is 2.5 m in all directions and the time step is 0.025 s. Computations are carried out for approximately 90 minutes of real time. The velocity perturbations upstream of the turbine are obtained from a pre-generated turbulent wind field (see [14]). The magnitude of the fluctuations were scaled in order to mimic three different incoming turbulence intensity (0%, 3%, 10%). Out of 90 minutes long flow simulations, 20 minutes data are used for each turbulence intensity case to feed in the acoustic simulations. The flow was maintained using body forces that are calculated with prescribed boundary layer method. The inflow wind profiles were determined using the classical power law exponent approach: $U(z) = U_{hub} \cdot \left(\frac{z_{hub}}{z}\right)^{\alpha}$ where the hub height velocity is set to 8 m/s and the power law coefficient (α) is set to 0.14, 0.3 and 0.45.

For the upwind propagation a frozen turbulence approach is employed. A large domain of synthetically generated turbulence was superposed with various inflow wind profiles and convected with the mean flow. This assumption surely has certain limitations however the scattering towards the shadow zones that are seen at the upwind propagation of sound waves will still be captured.

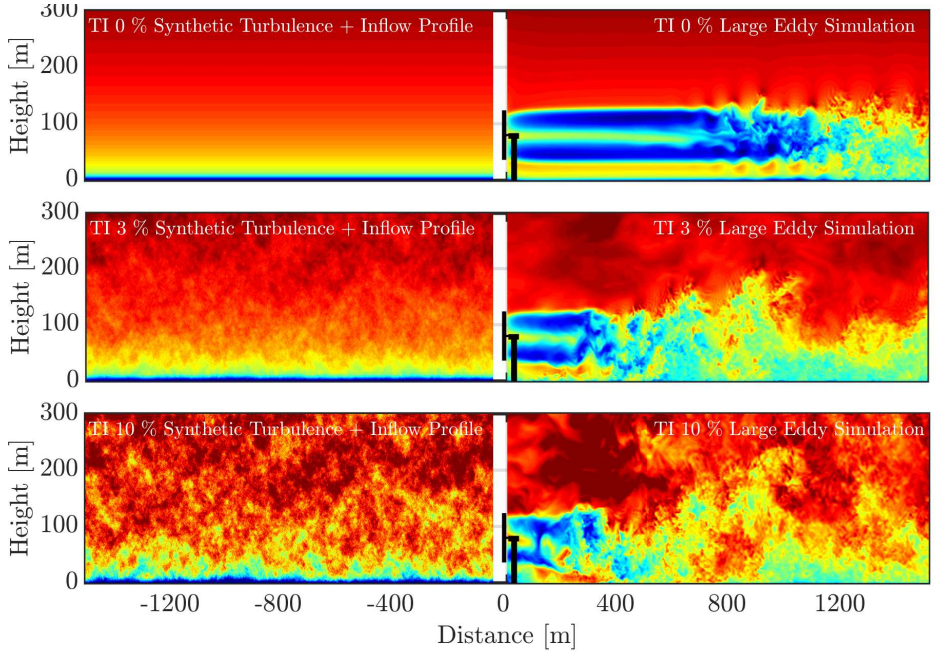

Figure 2. Snapshots of the streamwise velocity that are used as input to the PE model. **Left:** Superposition of inflow profile and a synthetic turbulent field; **Right:** LES output; **From top to bottom:** Increasing the turbulence intensity (0%, 3%, 10%)

3. Results

3.1. Effect of Wind Shear and Turbulence on Time-Averaged SPL

Wind shear is an important factor for the noise generation and propagation both downwind and upwind of a wind turbine. Downwind propagation is influenced by the shear due to two reasons: a) the wake development changes with wind shear b) higher wind shear results in a more continuous downward refraction. Additionally, wind shear creates periodic change of inflow angle which is related to SPL modulation. Upwind propagation is also influenced because higher shear values will result in a more severe upward refraction. This changes the locations of the initial ground reflection as well as the shadow zones (regions with low level noise). These effects are clearly visible in Fig. 3 which shows the time averaged sound pressure levels under various flow conditions. The shadow zone upwind of the wind turbine starts closer to the source with increasing wind shear. Noise levels for higher wind shear cases are lower for distances larger than 800 m. As for the downwind propagation it is important to remember the flow fields in Fig. 2. For 0 % turbulence intensity case the wake breakdown location depends predominantly on the wind shear. Higher wind shear results in earlier breakdown, subsequently the downwards bursting zones appear closer to the source. These regions for a receiver height of 2 m can be more clearly seen in Fig. 4 (800 m for $\alpha = 0.45$, 1200 m for $\alpha = 0.14$). Furthermore, higher turbulence level causes wind shear to lose its importance, because the initial wake instability is caused by the

incoming turbulence. For example, for the 10 % case the SPL differences between the three wind shear cases are hardly distinguishable. More importantly, the incoming turbulence influences the source power levels because of the contribution from turbulent inflow noise. The increase in these levels (particularly in the low frequency region, see Fig. 1) is directly effective on the far field noise. This is easily seen in Fig. 4 for both upwind and downwind propagation. Especially the 10 % case has significantly higher levels. The difference between 10 % and 3 % reaches up to 8-9 dB at around 700 m distance downwind of the wind turbine, while these values are even higher for the 10 % and 0 % difference (11-12 dB).

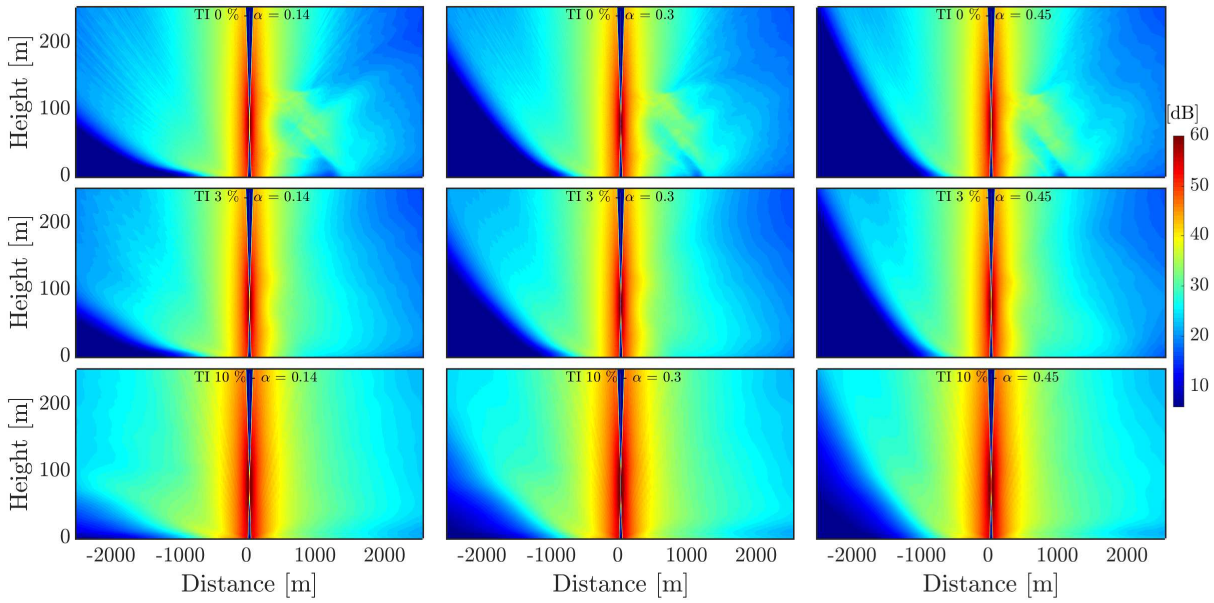

Figure 3. Time-averaged contours of SPL under various flow conditions. Source located at 0 distance and incoming flow direction is from left to right. **From top to bottom:** Increasing the turbulence intensity (0%, 3%, 10%); **From left to right:** Increasing wind shear coefficient (0.14, 0.3, 0.45)

Another observation that can be deduced from these plots is that the sound pressure levels at the upwind of the wind turbine reaches higher values than the downwind case at certain distances i.e. 200 m - 500 m. This is shown in the inner plot of Fig. 4. This is an interesting observation indicating that it takes longer distances before the atmospheric conditions start being effective on the sound propagation from an elevated source (in this case a wind turbine). With this in mind, we can conclude that upwind propagation should also be considered for the noise mapping tools, if the investigated distances are less than 800 m. Nevertheless it is clear that the far field noise levels at the upwind of a wind turbine (above 800 m) is considerably less than the downwind case.

3.2. Near and Far Field SPL Modulation

As mentioned in the introduction the unsteady nature of the wind turbine noise causes annoyance. In this section, via observing the time evolution of the sound pressure levels the modulation characteristics are investigated under various flow conditions. Fig. 5 shows the surface plots for three revolutions. In order to simplify the comparison we will focus on four regions that are indicated with the dashed lines namely, 1D, 6D (also referred as near field) and

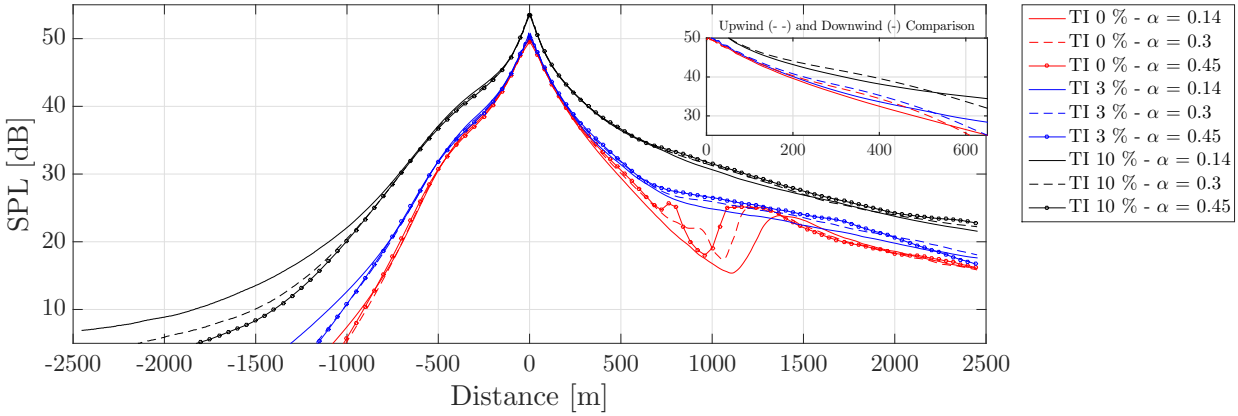

Figure 4. Time-averaged SPL under various flow conditions for a receiver height of 2 m. Source located at 0 m distance and incoming flow direction is from left to right.

12D, 25D (also referred as far field). The focus is on modulation depth, which is described as the maximum peak-to-trough ratio over one rotation in this study.

It is observed that at 1D all cases have similar behaviour. The modulation depth has values of 3-4 dB. The overall levels increase with increasing turbulence, however the modulation depth values remain similar. This is the region where the movement of the source is the dominating factor for the modulation. Additionally the spectra plots (not shown here) reveals that in the near field all frequency ranges have similar effects on the overall noise levels. This means increase in the high frequency content would be as important as the increase in low frequency content of the source power level. This changes with increasing distance as the atmosphere absorbs the high frequencies more than the low ones. Thus we can conclude that the low frequency content is more emphasized in the far field. At 6D region the modulation depth decreases with increasing turbulence. This is due to the fact that turbulence results in coherence loss and scattering of the sound waves propagating from source to receiver. Thereby the SPL time signal has a more smeared behaviour. Hence the peak to trough ratios decrease.

At 12D region the effect of wind shear is more visible in comparison to the near field (1D and 6D), especially for the downwind propagation and for the low turbulence intensity case. This is due to the effect of wake deficit and how it changes in different wind shears. In this region (12D) the modulation depth for upwind propagation have similar values, even though the overall levels vary with respect to turbulence intensity. In other words the mean atmospheric characteristics are taking over the propagation phenomenon.

At 25D region the sound pressure levels for upwind propagation are negligibly low, especially for 0% and 3% cases. However the modulation depth values are very much shear dependent. This is both due to the strong upwards refraction and periodic change of the source SPL as the effect of wind shear.

In addition to the overall time signals we also investigated the frequency dependent standard deviation values. The results (see Fig 6) show certain regions with significantly high levels. For the upwind propagation these regions are results of the moving source which causes a constant variation of the shadow zones (i.e. a receiver at 700 m may hear a lot of noise at one instant and at another instant the receiver hears nothing). This ideal picture is only valid for 0 % case, hence the region with high standard deviation is very large and distinct. With the increasing turbulence these regions become narrower and they are followed by the regions with standard deviation values of 5 dB - 6 dB. This is due to turbulence scattering to the shadow zones. These

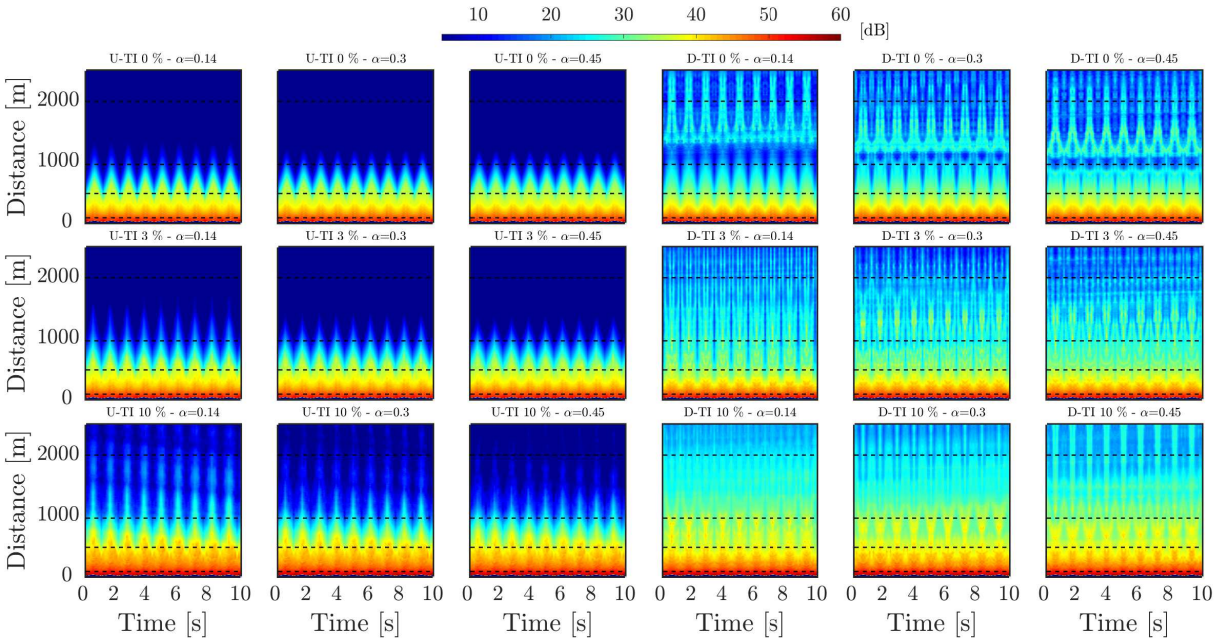

Figure 5. Time-evolution of SPL under various flow conditions for a receiver height of 2 m. **From top to bottom:** Increasing the turbulence intensity (0%, 3%, 10%); **From left to right:** Upwind (U) and downwind (D) propagation with increasing wind shear coefficient (0.14, 0.3, 0.45)

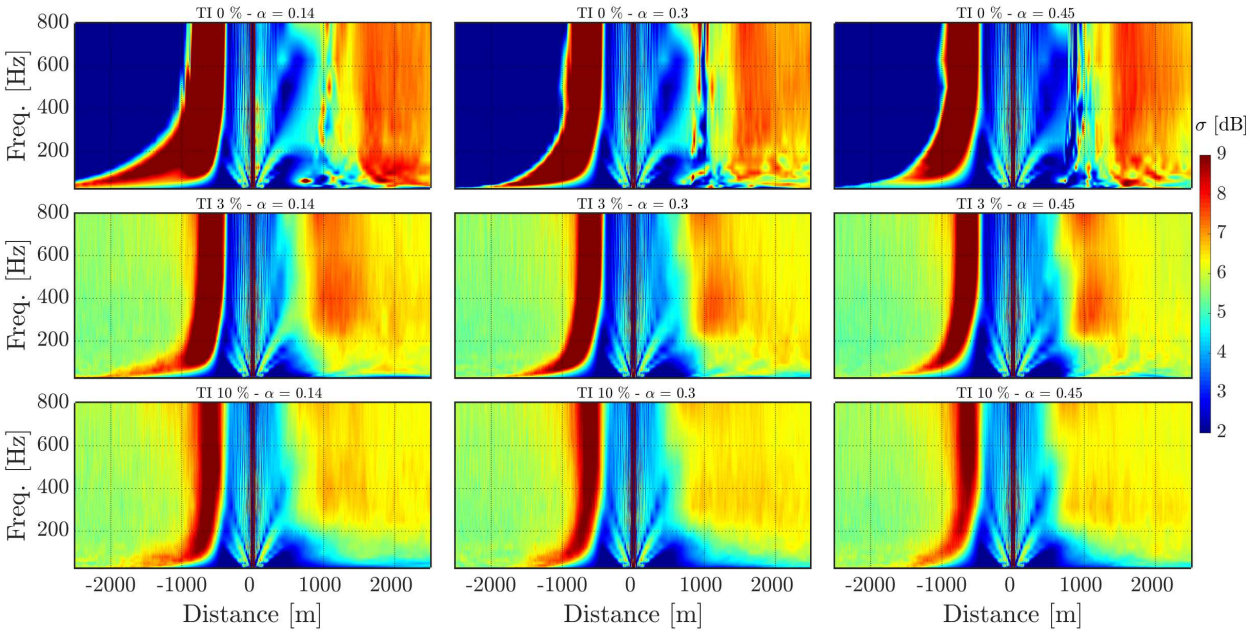

Figure 6. Frequency dependent standard deviation of SPL for a receiver height of 2 m under various flow conditions. **From top to bottom:** Increasing the turbulence intensity (0%, 3%, 10%); **From left to right:** Increasing wind shear coefficient (α=0.14, α=0.3, α=0.45)

levels increase with increasing turbulence. This behaviour is similar for all upwind cases. It is observed that the lower the frequency, the further the start of the shadow zone. Thus the increased levels of standard deviation are visible for longer distances. This distance varies with wind shear. This behaviour is in agreement with the previous ones, which we explained with the fact that low frequencies propagates much longer distances before they are affected by the atmospheric conditions.

While a general trend can be deduced for the upwind propagation results, each downwind propagation case has a different SPL development. For 0 % case until the wake breakdown the standard deviation values are relatively low (2-3 dB). As the wake breaks down the sound waves, that are ducted within the wake, are refracted towards the ground. Similar to the upwind case with the moving source these regions show high variation. Thus there is a sudden increase of the standard deviation values just around the wake breakdown regions. The start of these regions vary with wind shear. For the two higher turbulence intensity cases, it is observed that the SPL standard deviation values for TI=3 % are either equal to or higher than TI=10 %. This can again be explained with the wake evolution. The wake deficit for 3 % case is longer than the 10 % case. This means the sound waves emitted from the source will be ducted within the wake deficit and eventually will be refracted downwards. As the source moves up and down this regions become more and less noisy, hence the standard deviation values are higher.

3.3. Investigation of SPL Modulation due to Wake

In this last part, we take a closer look at the frequency dependent downwind propagation in order to investigate SPL modulation caused by the wake deficit. We have carried out 16 minute long acoustics propagation simulations using the LES as the flow input that is sampled at 10 Hz. This yields 10000 data points in time, for each frequency (in total 15 of them between 31.5 Hz - 800 Hz), each flow condition and for all distances for a receiver at 2 m height. In addition to the directly LES coupled PE (referred as LES+PE), we conducted another set of simulations using the fluctuations obtained by subtracting the average flow field from each LES snapshot and using this as PE input. This method is referred as Perturb+PE because the flow field input only contains the wake induced perturbations. Thus the effect of the main wake deficit is disregarded.

In order to quantify the modulated energy difference between LES+PE and Perturb+PE we followed a certain procedure for each frequency. Fig. 7 shows the sample steps for this procedure. First of all, time dependent acoustic signals are converted into Fourier space via 1D FFT. This yields a spectrum for each distance, for each acoustic frequency, for each flow condition and for each method (LES+PE and Perturb+PE). Subsequently these are subtracted from each other. This methodology allows us to detect certain regions where the modulation caused by the wake deficit is higher or lower in comparison to the modulation caused by the perturbations.

Using the differential spectra plots (not shown here) certain observations were made that are listed below:

- For a low frequency, i.e. 31.5 Hz, the difference between LES+PE and Perturb+PE is distributed over a wide range of propagation distance. At a higher frequency, i.e., 800 Hz, differences are mainly seen in narrow region.
- For the different turbulence intensity cases, it is seen that wake effect is more pronounced at lower TI. With a high TI, wake is shortly merged with ambient turbulence, thus less difference is observed at high TI cases.
- Wind shear variation also makes a clear difference. For each acoustic frequency and for each turbulence intensity, the increase of shear factor results in a larger difference.

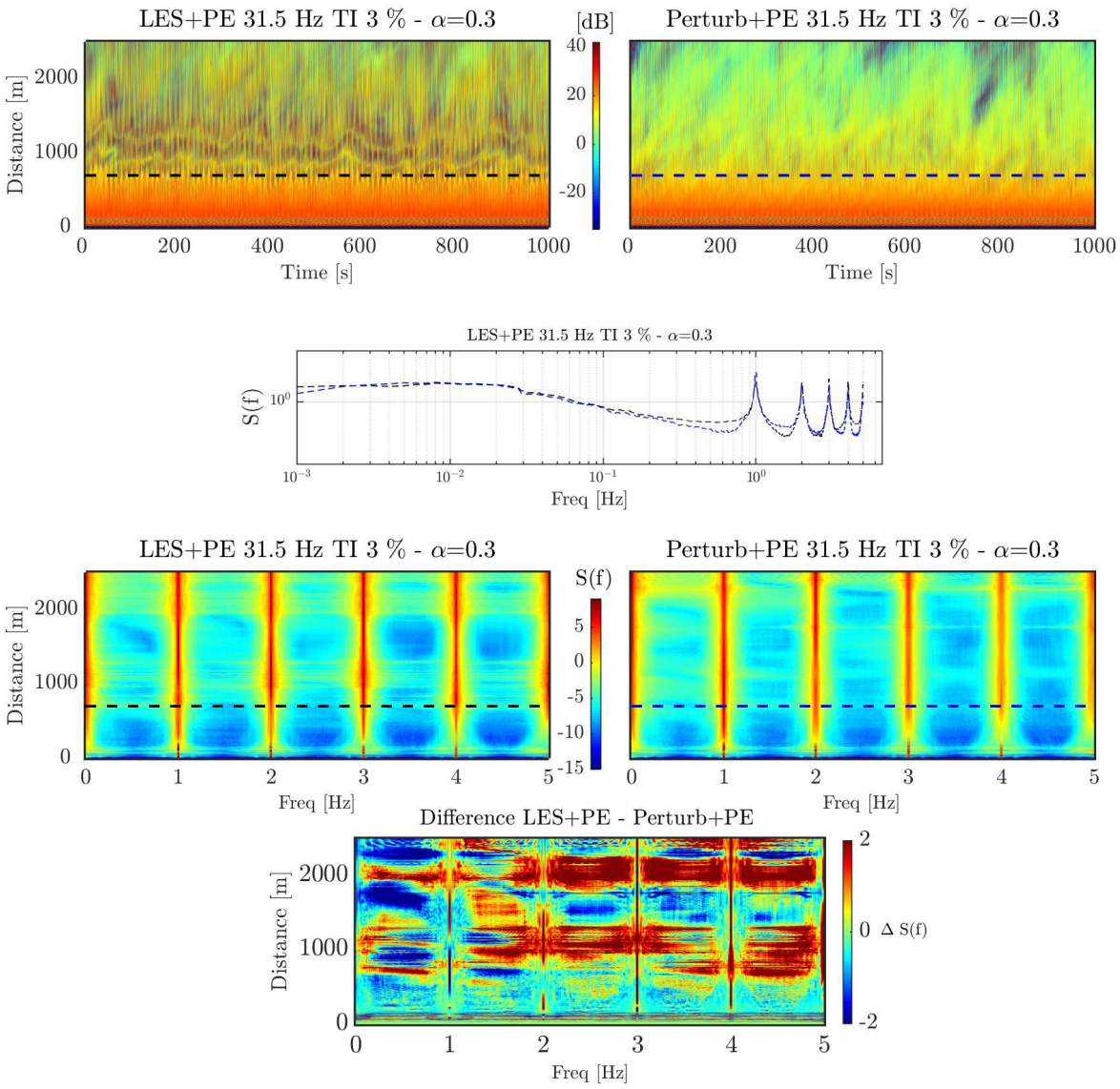

Figure 7. Explanation of the modulation quantification procedure. Sample time-distance signal of an acoustic frequency of 31.5 Hz for a receiver at 2 m height, converted to Fourier space for both methods (LES+PE and Perturb+PE) subsequently subtracted

4. Conclusions

In this paper we underline the effects of the atmospheric conditions (wind shear and turbulence) on wind turbine noise generation and propagation mechanisms. Considerable effects are observed for time-dependent as well as time-averaged sound pressure levels at the far field receiver locations. The effects on the time-averaged SPL can be summarized in two reasons. First of all, higher ambient turbulence intensity results in increased sound source power levels, particularly at the low frequency content (31.5 Hz - 300 Hz). This directly affects the far field noise (up to 2500 m), as the atmospheric absorption is negligible for this frequency range. To the authors' knowledge none of the noise mapping tools take into account the increased source levels due to

ambient or wake induced turbulence. Neither the standards demand turbulence dependent noise curves. We believe that this can be one of the reasons for inaccurate far field noise predictions.

Second of all, it is observed that under low incoming turbulence the wind shear has significant effect on downwind propagation. This effect loses its importance with increasing turbulence. This is because turbulence is the dominating factor for the wake deficit evolution, therefore the sound wave refraction patterns. On the other hand, for the upwind propagation the wind shear has consistently the same effect. Regardless the turbulence intensity shadow zones start closer to the source, under higher wind shears. But turbulence cause insonification of these zones due to scattering. Another important observation is the SPL difference between upwind and downwind propagation. Expectedly, the far field (above 900 m) noise levels for upwind propagation were much lower than the downwind case. However, the results also showed that at certain near field distances (200 m - 500 m) the levels of the upwind propagation was higher than the downwind case. Most of the noise mapping tools consider only the downwind propagation as the worst case. Again this may be another reason for inaccurate noise mapping.

Through the time-dependent SPL analysis we showed that the SPL modulation close to the turbine (up to 250 m) has similar behaviour under all flow conditions. It is also important to underline that in these regions the high frequency content of the source power level is as important as the low frequency one. As the propagation distance increases the turbulence and wind shear effects become more important. For upwind propagation increased turbulence results in less modulation depth, because of the scattered waves to the shadow zones. For the downwind propagation, dependent on the distance from the source the wind shear and turbulence intensity either increases or decreases the modulation depth. It is not easy to conclude one trend however we observed clearly that these two factors are important for far field amplitude modulation.

Further investigation of the SPL modulation due to wake deficit showed that particularly the low incoming turbulence levels (0 % and 3 %) result in increased spectral energy of the low acoustic frequency content over wide spread propagation distances. This can lead to beating noise at far field.

With this study we emphasize the importance of these issues in order to predict the farfield wind turbine noise accurately. Further work will be carried out on more consistent coupling of the wind turbine noise generation and propagation models as well as the extension of these for wind farms.

Acknowledgments

The work has been funded by the GreenTech Wind project, a collaboration of the EuroTech Universities.

References

[1] Smith M, Bullmore A, Cand M and Davis R 2012 Mechanisms of amplitude modulation in wind turbine noise Societe Francaise d'Acoustique Acoustics Nantes France.
[2] Large S and Stigwood M 2015 Compliance isn't everything 6th International Meeting on Wind Turbine Noise Glasgow
[3] Barlas E, Zhu J W, Shen W Z, Kelly M C and Andersen S J 2016 Effect of Wind Turbine on Atmospheric Sound Propagation, Applied Acoustics (under review)
[4] Ostashev V E, Juve D and Blanc-Benon P 1997 Derivation of a wide-angle parabolic equation for sound waves in inhomogeneous moving media Acta Acustica united with Acustica Vol 83 Number 3 May/June 1997 p 455-460(6)
[5] Delany M E and Bazley E M 1970 Acoustical properties of fibrous absorbent materials. Applied Acoustics (3), 105116.
[6] Zhu W J, Heilskov N, Shen W Z and Sørensen J N 2005 Modeling of Aerodynamically Generated Noise From Wind Turbines J Sol Energy Eng 127(4), 517-528
[7] Oerlemans S, Sijtsmaa P and Mendez Lopez B 2007 Location and quantification of noise sources on a wind turbine Journal of Sound and Vibration Vol 299 p 869-883

[8] Michelsen J A 1992 Basis 3DA Platform for Development of Multiblock PDE Solvers, AFM 92-05 Technical University of Denmark
[9] Sørensen N N 1995 General Purpose Flow Solver Applied to Flow over Hills, Ph.D. thesis Technical University of Denmark
[10] Sørensen N N 2002 Numerical Modeling of Wind Turbine Wakes Journal of Fluids Engineering Vol 124 p 393-399
[11] Øye S 1996 Flex4 simulation of wind turbine dynamics, Proceedings of 28th IEA Meeting of Experts Concerning State of the Art of Aeroelastic Codes for Wind Turbine Calculations. Available through Int
[12] Sørensen J N, Mikkelsen R F, Henningson D, Ivanell S, Sarmast S and Andersn S J 2015 Simulation of wind turbine wakes using the actuator line techniquemPhil. Trans. R. Soc. Aernational Energy Agency
[13] Madsen H A, Bak C, Paulsen U S, Gaunaa M, Fuglsang P, Romblad J, Olesen N A, Enevoldsen P, Laursen J and Jensen L 2010 The DAN-AERO MW Experiments,Danmarks Tekniske Universitet, RisøNationallaboratoriet for Bredygtig Energi
[14] Mann J 1998 Wind field simulation, Probabilistic Engineering Mechanics, vol 4 pg 260-282